Multianalyte Physiological Microanalytical Devices

Anna Nix Davis,[1] Adam R. Travis,[1] Dusty R. Miller,[1] and David E. Cliffel[1,2]

[1]Department of Chemistry, Vanderbilt University, Nashville, Tennessee 37235; email: d.cliffel@Vanderbilt.edu

[2]Vanderbilt Institute for Integrative Biosystems Research and Education, Vanderbilt University, Nashville, Tennessee 37235

Annu. Rev. Anal. Chem. 2017. 10:93–111

The *Annual Review of Analytical Chemistry* is online at anchem.annualreviews.org

https://doi.org/10.1146/annurev-anchem-061516-045334

Keywords

multianalyte physiometry, multiplex, electroanalytical, biosensor, multielectrode arrays, microclinical analyzer

Abstract

Advances in scientific instrumentation have allowed experimentalists to evaluate well-known systems in new ways and to gain insight into previously unexplored or poorly understood phenomena. Within the growing field of multianalyte physiometry (MAP), microphysiometers are being developed that are capable of electrochemically measuring changes in the concentration of various metabolites in real time. By simultaneously quantifying multiple analytes, these devices have begun to unravel the complex pathways that govern biological responses to ischemia and oxidative stress while contributing to basic scientific discoveries in bioenergetics and neurology. Patients and clinicians have also benefited from the highly translational nature of MAP, and the continued expansion of the repertoire of analytes that can be measured with multianalyte microphysiometers will undoubtedly play a role in the automation and personalization of medicine. This is perhaps most evident with the recent advent of fully integrated noninvasive sensor arrays that can continuously monitor changes in analytes linked to specific disease states and deliver a therapeutic agent as required without the need for patient action.

1. INTRODUCTION

The development of analytical devices incorporating sensors for multiple analytes has enabled new studies of physiological systems. For example, although electrochemical glucose sensors (1–3) have a well-established clinical presence in monitoring patients with diabetes (1) and pre- and postoperative surgical patients (4), fundamental studies on aerobic and anaerobic respiration are better accomplished through the detection of lactate, oxygen, and pH in addition to glucose (**Figure 1**) (5). When observing physiological effects with complex methodologies, ranging from monoculture microfluidic devices to clinical samples, sensing strategies often need small devices to accommodate limited patient sample volume while providing moderate-throughput experiments.

The subfield of multianalyte physiometry (MAP) has emerged to broaden the understanding of physiological pathways with multianalyte analysis using either a sensor array or single multiplexed detector to probe complex biochemical processes in higher dimensions (spatial and temporal) of phase space. Researched applications of electrochemical MAP sensors include observations of biological and chemical responses to stimuli, determination of the health status of organs on chips (OOCs), and development of novel clinical and point-of-care (POC) devices for vivo/in situ research. When approaching the more complex task of detecting multiple analytes in living organisms, implantable ultramicroelectrodes decrease the disruption in animal models when compared to larger microdialysis probes or electrode arrays. Combining this with fast-scan cyclic voltammetry (FSCV) can yield submicrometer spatial resolution and subsecond temporal resolution (6, 7). The demand for minimally invasive devices to manage chronic conditions has resulted in numerous wearable devices. These wearable devices are capable of monitoring different analytes simultaneously and continuously, interfacing with mobile phones, and delivering a therapeutic agent (**Table 1**).

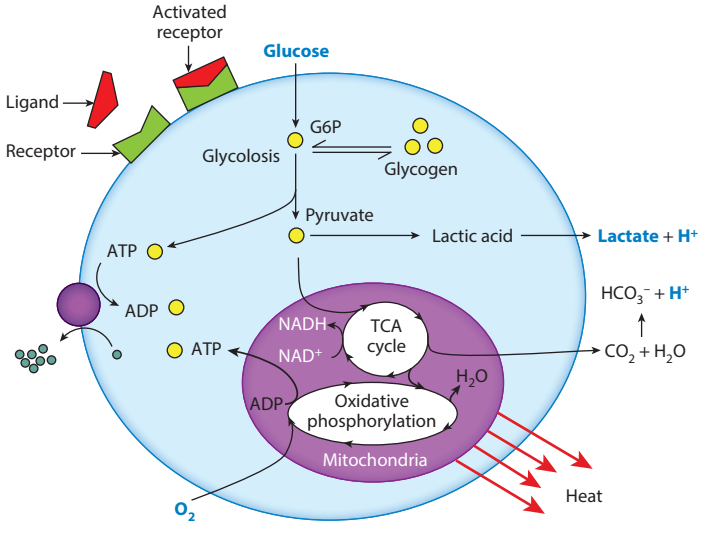

Figure 1

Schematic of a cell showing cellular bioenergetics pathways. Metabolites commonly detected with multianalyte physiometry (lactate, glucose, oxygen, and acid) are highlighted. Abbreviations: ADP, adenosine diphosphate; ATP, adenosine triphosphate; G6P, glucose 6-phosphate; NAD, nicotinamide adenine dinucleotide; NADH, nicotinamide adenine dinucleotide hydrate; TCA, tricarboxylic acid. Adapted with permission from Reference 10. Copyright 2006, Elsevier.

Table 1 Summary of physiological systems and their multianalyte readouts in microanalytical devices

Systems	Analytes/event detection method	References
Cellular bioenergetics	Glucose, lactate, oxygen, pH, ATP	5, 9–18, 20, 21, 23, 24, 41
Oxidative stress	RNS, ROS, glutathione, AA, Tyr	36–39, 42
Vesicular exocytosis	Histamine, dopamine, serotonin	29, 31, 32
Antioxidant capacity	Caffeic, gallic, ascorbic, and trolox T acids	34, 35, 43
Neurotransmitters	Dopamine, adenosine, serotonin	32, 33, 40, 42
Cytotoxicity	K^+, Na^+, H^+, Ca^{2+}	28
Patient monitoring and diagnosis	Ions, biomolecules, glucose, urea	47, 58, 59, 67, 70

Abbreviations: AA, ascorbic acid; ATP, adenosine triphosphate; RNS reactive nitrogen species; ROS, reactive oxygen species; Tyr, tyrosine.

2. IN VITRO MICROFLUIDIC STUDIES

Multianalyte physiological microanalytical devices encompass many experimental methodologies and devices. Electrochemical measurements within a microfluidic device, where the electrode sensors are built within a self-contained system, are the focus of this section. Examples of these devices and methods include microphysiometers, microclinical analyzers (MCAs), microfluidic electrophysiology, multielectrode arrays, and microchip electrophoresis (ME) coupled to electrochemical detection. Each of these subtypes is reviewed in the sections below.

2.1. Multianalyte Microphysiometer

Conventional microphysiometry was developed by Harden McConnell and coworkers and led to the Cytosensor Microphysiometer from Molecular Devices (8), an instrument that measured the extracellular acidification (i.e., pH changes) produced by the metabolism of approximately 100,000 to 1,000,000 live cells in a 3-μL microfluidic chamber using light-addressable potentiometric sensors (**Figure 2*a***). This cytosensor has been modified (**Figure 2*b***) into the multianalyte microphysiometer (MAMP) to detect glucose, lactate, and oxygen in addition to pH inside the cell chamber. These additional analytes are detected amperometrically: Oxygen is directly detected, whereas immobilized glucose oxidase and lactate oxidase detect glucose and lactate, respectively (**Figure 2*b***, **Table 1**) (5, 9–17). The MAMP has been used to investigate the metabolic effects of nutrient concentrations on cellular bioenergetics (13), chemical toxins (5, 9–12), harmful proteins (11, 12), noninvasive fluorescent chemical probes (14), and oxidative burst (15–19). Major shifts in cellular bioenergetics observed in the MAMP have also demonstrated shifts in the utilization of aerobic or anaerobic respiration pathways (5, 9).

Multiplexing cellular bioenergetics and insulin detection can offer valuable information on the complicated physiology and metabolism. For example, excised pancreatic islet physiology and metabolism were studied by combining an insulin-selective electrode with the aforementioned MAMP electrodes. This allowed the time-dependent study of insulin release resulting from a hyperglycemic environment (20).

Cellular bioenergetics studies of neurons using the MAMP have revealed a strong correlation between neuronal adaptation and survival that results in the development of a new model of transient ischemic attack (TIA) (13). In general, metabolic adaptation to stress is critical for cell survival but is poorly understood. Experiments using the MAMP have revealed metabolic compensation; therefore, survival of nutrient-deprived neurons relies on neuronal-glial chemical and physical

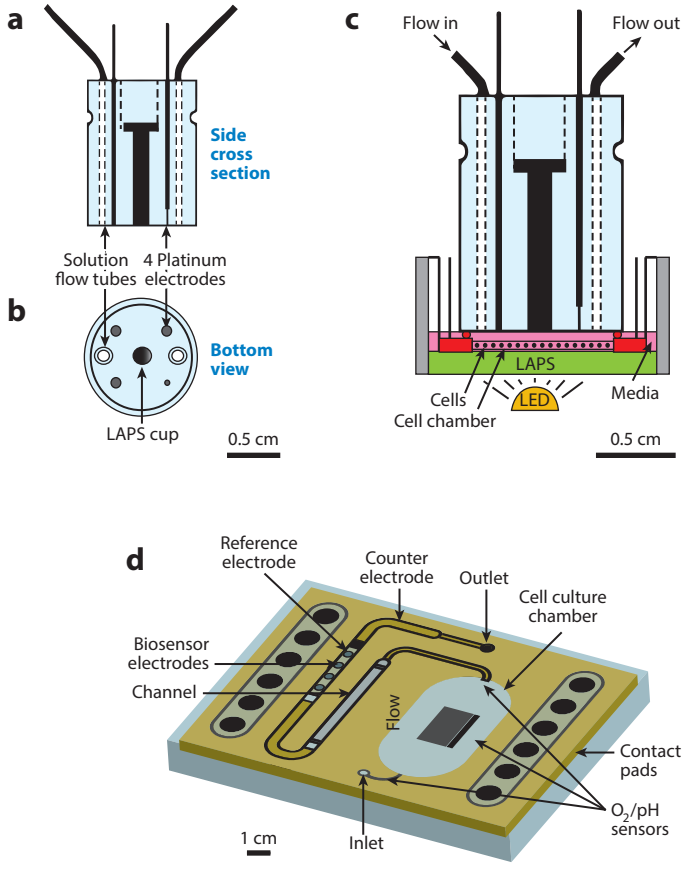

Figure 2

Multianalyte physiometers. (*a*) Side cross section and (*b*) bottom view of a Cytosensor™ modified into a multianalyte microphysiometer by electrode addition. The four added platinum electrodes include three working electrodes and one counter electrode. The working electrodes detect glucose, lactate, and oxygen. Panels *a* and *b* adapted with permission from Reference 5. Copyright 2004, American Chemical Society. (*c*) Samples are stop-flowed into the device, and pH is measured through light-emitting diode (LED)-illuminated light-addressable potentiometric sensors (LAPS). Panel adapted with permission from Reference 10. Copyright 2006, Elsevier. (*d*) Schematic of a multianalyte physiometer based on a glass chip that combines a cell cultivation chamber, microfluidics, and metabolic monitoring. Oxygen and pH are measured in the cell culture area, and biosensors for lactate and glucose are connected downstream by microfluidics. The wafer-level fabrication features thin-film platinum and iridium oxide microelectrodes on a glass chip, microfluidics in an epoxy resist, a hybrid assembly, and an on-chip reference electrode. Panel adapted with permission from Reference 21. Copyright 2014, Royal Society of Chemistry.

communication. This model of TIA was tested with primary neurons primed with short deprivations of oxygen and glucose in the days leading up to an otherwise lethal deprivation. When primed, neurons achieved increased survival rates over unprimed neurons (22). After priming the neurons, consumption of cellular adenosine triphosphate (ATP) and neuronal oxygen increased above baseline. After these primed neurons were treated with oxygen deprivation triggering an anaerobic pathway shift that would normally be lethal to the neurons, these primed neurons recovered normal lactate production within 30 min. The corresponding rapid increase in aerobic respiration (monitored via oxygen consumption) observed after priming, coupled with the increase in cellular ATP,

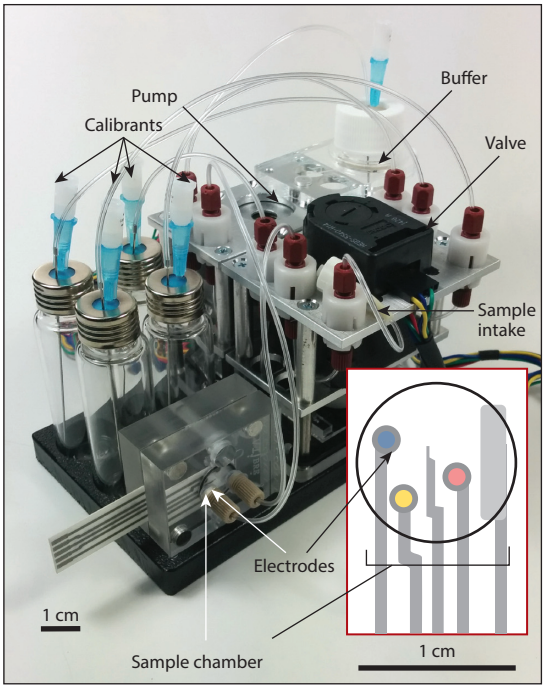

Figure 3

Photograph of a microclinical analyzer inset with a schematic of a screen-printed electrode. The pump and valve work together to flow 26 μL of buffer, calibrants, and/or sample into the sample chamber containing the electrodes. From left to right, electrodes are modified to detect pH (*blue*), glucose (*yellow*), oxygen (*middle*), and lactate (*pink*). The far right electrode is an Ag/AgCl quasi-reference. Photograph courtesy of Dmitry Markov.

indicates that the protective pathways in this ischemic model include the immediate increase in the production of energy stores through aerobic respiration. The increase in energy production may help to prevent cellular starvation upon subsequent stress. This provides the first dynamic measurement used to identify essential events mediating neuronal injury in vitro and can aid in the identification of predictive biomarkers in injury. The microphysiometry data reveal that the greatest single predictor of neuronal survival is extracellular acidification; however, lactate levels, which are currently key clinical indicators of injury, were not in fact correlated with neuronal cell fate (13, 23).

2.2. Microclinical Analyzer

Unlike in multianalyte microphysiometry, where the sensors are embedded in the microfluidic cellular chamber, in an MCA the electrochemical measurements are performed in a separate chamber downstream (**Figure 3**). Thus, MCA measurements can be multiplexed between multiple OOCs using a valve to select which organ effluent is to be measured. Thus, the MCAs trade temporal and spatial resolution for increased resistance to biofouling of the electrochemical sensors. The MCA is a self-calibrating device consisting of a microfluidic pump and valve that direct calibrant and sample solutions to a 26-μL sample chamber, where an array of platinum screen-printed electrodes (SPEs) amperometrically detects hydrogen peroxide (H_2O_2) produced by spatially separated enzyme films and potentiometrically detects pH via open-circuit potential shifts using electrodeposited iridium oxide. SPEs are robust, highly reproducible, and low cost,

resulting in a device that is easily customizable with interchangeable sensors capable of measuring glutamate, acetylcholine, calcium, potassium and/or sodium (19, 24). Custom multichannel potentiostats were created to accommodate simultaneous MCA measurements (25). The Cliffel lab's investigations with the MCA instrument have focused on monitoring tissues and OOCs (26, 27).

Other researchers have developed similar MCAs that have been used in toxicological testing of healthy and cancerous cells (21, 28). Running multiple simultaneous experiments with multisensor microsystems allows for a moderate-throughput screening of potential drug candidates (21). An electrolyte-focused MCA was developed with four ion selective and three partially selective electrodes that were selective for potassium, sodium, hydrogen, calcium, amines, cations, and anions. These electrolyte MCAs are primarily associated with signaling flux from ionic gradients. Although pathway elucidations are not always exact using chemometric analysis, training sets can be used to define a particular physiological state of interest. This combination of electrolyte sensing and multiplexed analysis was used to determine the ratio of dead-to-live cells in a cancer therapeutics screening (28).

2.3. Electrophysiological Event Monitoring

Exocytosis of redox active species can be measured potentiometrically or amperometrically (29) and has led to numerous discoveries in vesicle transport (29–33). For example, measurements of the relative concentrations of specific analytes, including octopamine, following release were reported (30). Although it is not always possible to differentiate the molecules released, the timing and frequency of events marked by the release of neurotransmitters have been recorded (31), and microelectrode arrays allow for both single-cell and population analyses (32). Additionally, the initial pore size before full release has been mathematically modeled using experimentally determined parameters (31). Nanopipette potentiometric electrodes and carbon fiber nanoelectrodes can be used separately or in combination to measure postsynaptic potential shifts and neurotransmitter release events (29, 31, 33). Measurements of synaptic events were performed in a microfluidic device that cocultured superior cervical ganglion neurons and smooth muscle cells (**Figure 2*c***) to confirm that synaptic events mimic in vivo conditions in addition to improved axon orientation (31). The device architecture seals the chamber for oxygen detection and decreases the media volume, increasing the sensitivity to pH, which can be measured through the bottom glass plate.

2.4. Multiplexed Sensing of Reactive Oxygen and Nitrogen Species

Oxidative stress is marked by the production of reactive oxygen species (ROS) and reactive nitrogen species (RNS), specifically H_2O_2, nitric oxide ($NO^{\cdot}$), nitrite (NO_2^-), and peroxynitrite ($ONOO^-$). By amperometrically measuring at four different potentials, the concentrations of ROS and RNS can be determined using a physiological model consisting of four linear equations delimiting the current contributions of each compound. The detection of ROS and RNS concentrations has been used to quantify antioxidant capacity, determine the basic cellular function of macrophages, and compare the effectiveness of cancer therapies. The antioxidant capacity of a superoxide dismutase mimicking manganese complex (34) was determined by amperometric detection of ROS and RNS produced by macrophages. An electrochemical microfluidic device simulates the redox effect of ROS constituting a new cell-free method for determining antioxidant properties (35). This method was tested with trolox, ascorbic acid (AA), gallic acid, and caffeic acid, which are compounds with known antioxidant properties. In a study of a macrophage's ability to control ROS and RNS release and implement protective measures, two platinum electrodes were used to observe the dynamic concentrations of intracellular and extracellular ROS and RNS. By inserting and sealing

one electrode into a macrophage while simultaneously measuring outside the same cell, ROS and RNS leakage through phagolysosomes and neutralization to avoid premature oxidative damage was observed (36). Experimental drugs of the ferrocifen class were tested on two breast cancer cell lines to determine how treatment with each affected mechanical depolarization of the cells. As the multiplexed detection of ROS and RNS species allows for the concentration of each species to be quantified, the analysis of each drug's effectiveness showed that H_2O_2, $NO^{\cdot}$, NO_2^-, and $ONOO^-$ production was not uniformly affected, yet the differences in the mechanism of action require more study (37). After being established, the multiplexed amperometric detection of ROS and RNS at four potentials was integrated into a microfluidic device that separates each analytical measurement into individual 38-μL cell chambers (38).

2.5. Microchip Electrophoresis with Amperometric Detection

As an alternative approach to multielectrode formats, ME methods have been applied to MAP. By adding a separation step prior to electrochemical detection, these devices can increase the number of analytes detected on a single electrode. One challenge in pairing ME and amperometric detection is noise from high ME operating potentials. However, noise reduction techniques, such as in-channel detection and an electrically isolated potentiostat, can be implemented (39). ME with amperometric detection (**Figure 2*d***) has been used to detect redox active biomolecules, interfering species that are electroactive at the same potentials as target molecules (39–47), and to detect glucose by using a glucose oxidase-modified working electrode (41). Methods have been optimized to observe NO production in macrophages stimulated with lipopolysaccharide by analyzing NO_2^- ions (42) and dopamine (DA) metabolites from rat brain slices (46). ME with amperometric detection is a versatile technique that can detect multiple analytes and does not require specific modification of each electrode sensor. This enables ME to be more generic, as the same basic device does not need specific analyte modifications to detect another set of species.

3. CLINICAL DEVICES AND TESTING

Clinical testing and POC devices incorporate MAP to monitor, diagnose, or treat a patient. With hundreds of possible tests available, clinical MAP devices focus on patient monitoring, organ function, or disease diagnosis. These focused assays significantly narrow the number and type of tests performed. Typically, a physician starts by monitoring a few dozen analytes in clinical blood tests during recovery, treatments, and procedures; they then transition to organ function and disease biomarker–specific tests if irregularities in the basic tests are present (48–50).

The i-STAT handheld blood analyzer (Abbott Point of Care; **Figure 4*a***) has been a staple in hospitals and doctors' offices worldwide for almost 25 years and is frequently a featured POC device in the clinical chemistry literature (48, 50–54). The self-contained testing cartridges have 19 commercially available variations that contain either single-analyte or multianalyte electrode arrays (48, 55). Low operating volumes (17–95 μL) accommodate comparative validation of a newly developed MAP device or improved detection schemes, especially if the amount of sample is limited. The cartridges contain a calibrant solution and one or more electrode arrays with exposed contact pads to easily connect to the handheld device. Quality control during the analysis includes a pseudosample statistical treatment to determine validity of the cartridge, followed by the sample, which is evaluated for concentrations, bubbles, and volume collected. If the calibrant and sample measurements meet the statistical demands, a digital output reports concentrations determined via single-concentration point calibration (48, 54). In most circumstances, pseudosample analysis is not ideal for treating data sets. To limit variability in the experimental conditions and determine

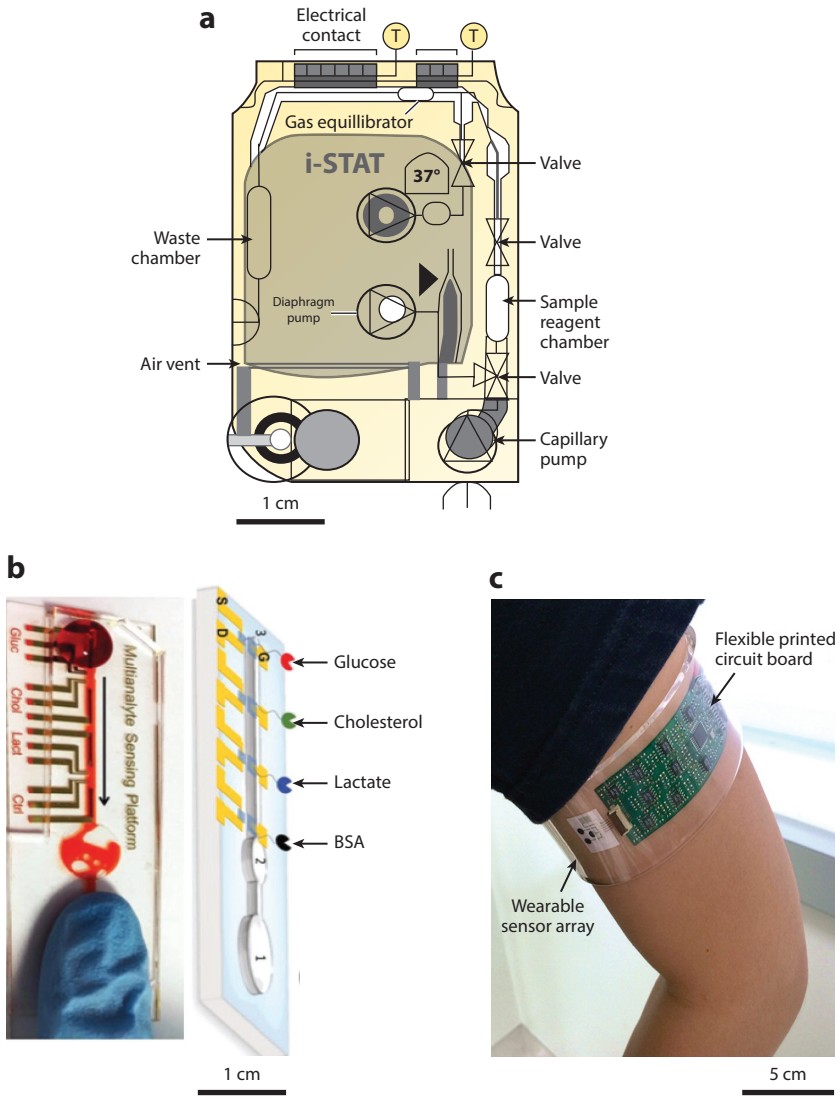

Figure 4

Clinical and wearable devices. (*a*) i-STAT handheld device. Adapted with permission from Reference 48. Copyright 1998, American Chemical Society. (*b*) Photograph and schematic of the selective multianalyte detection in complex media using the finger-powered OECT array. Photograph shows a red-colored solution that was pressure driven from the inlet through the sensing areas, as indicated by the vertical arrow. Adapted with permission from Reference 70. Copyright 2016, John Wiley & Sons. (*c*) A fully integrated wearable multiplexed sensing system on a subject's arm. Adapted with permission from Reference 91. Copyright 2013, Royal Society of Chemistry. Abbreviations: BSA, bovine serum albumin; OECT, organic electrochemical transistor.

data skews within the population, high-precision commercial microfabrication of cartridges and regular clinical chemistry evaluations are trusted (52–54, 56, 57). As a result of the reliability and immunoassay availability, an i-STAT device has been modified to detect point mutations in genetic diseases and differentiate viral and bacterial strains after an eight-minute on-device polymerase chain reaction (58). The small rugged nature of the i-STAT device lends itself to emergency room and POC use (53). Although the i-STAT has low operating volumes, it has not been the choice for OOCs and bioreactors because it lacks automated fluid handling and is targeted to physiometry measurements of samples 17 μL or larger.

3.1. Multiplexed Electrolyte Detection

A prominent category of physiological tests involves the monitoring of electrolytes, specifically sodium, potassium, calcium, magnesium, and chloride (48). Electrochemical ion detection is most commonly achieved via ion-selective electrodes (ISEs) and potentiometric techniques (25). Though many ion-selective membranes designed for ISEs are commercially available, innovative multiplexed, low-interferent, ion-selective sensors for ecological and physiological purposes could reduce the number of electrodes needed in an array, potentially leading to reduced detection volumes. Recently described layered devices utilized cyclic voltammetry to measure concentrations of multiple ions based on a thin membrane embedded with multiple ionophores covering an ion-to-electron transducing material. Ion transfer at the membrane surface occurs at specific potentials for different ions depending on the ionophore used (59–62). Although not all materials utilizing the thin membrane sensors are suitably robust for some biological samples, a recent polyurethane ionophore was able to detect lithium and potassium ions in a single scan in undiluted plasma and serum (61). ISEs enhanced with ion-exchange exclusion membranes have improved the separation efficiencies and sensor lifetimes, enabling them to be used in complex clinical samples (63–66). In addition to multiple electrolyte detection on a single sensor, fully automated ISE arrays have detected monoatomic and polyatomic ions for analysis of the carbon cycle in freshwater ecosystems (67).

3.2. Additional Biofluids

POC sensors need to handle measurements in various biological matrices, such as blood, cerebrospinal fluid, urine, intraocular fluid, and saliva, yet they function under a wide range of concentrations and interferents between these fluid types (49–51, 68, 94). New devices are being designed to avoid finger-stick blood draws by optimizing testing in fluids that require less invasive sampling (70, 94). One such MAP device was shown capable of measuring glucose, lactate, and cholesterol in blood and saliva with organic electrochemical transistors (**Figure 4*b***). In this device, analyte-specific oxidase enzymes were immobilized using chitosan modified with a ferrocene redox mediator onto poly (3,4-ethylenedioxythiophene):poly(styrene sulfonic acid) (PEDOT:PSS)-coated gold electrodes, which effectively lowered the operating potential to 100–200 mV and reduced the number of redox interferences. An additional electrode was included for the purposes of background subtraction where bovine serum albumin replaced the enzymes. The microfluidic flow of the sample through the device was controlled by manual compression of the housing (70).

4. IN VIVO MULTIANALYTE PHYSIOMETRY USING MICROANALYTICAL DEVICES

Because in vitro models do not reliably predict the efficacy of certain drugs in vivo, the need for animal and human trials remains. Several factors contribute to the discrepancy between predicted

versus observed therapeutic effects, including poor bioavailability of the compound and off-target toxicity of the drug or its metabolites. Although reductionist approaches have provided insight into the complex biochemical pathways that exist within the human body, it can be particularly difficult to predict off-target effects prior to in vivo testing. Additionally, the shift of the medical field toward personalized medicine makes it advantageous to develop methodologies that allow for continuous patient monitoring for an extended period of time.

4.1. Strategies for Avoiding Electrochemical Interference

Measurements made in undefined environmental conditions within an organism may encounter electrochemical interference. This interference can come either from direct sources, such as redox active species, or from indirect sources, such as biofouling. Interference commonly manifests as artificial changes in current or potential and can plague electrochemical investigations. The need to measure signal coming from only the analytes of interest has led investigators to develop several methods capable of reducing the impacts of electrochemical interference, including using electrostatic polymer barriers (6, 71–76), shifting the overpotential through electrode modifications (4, 77–81), and limiting electrode exposure time to the interfering species (82).

Polymer barriers, such as polypyrrole and Nafion films, can reduce the interference when making electrochemical measurements in vivo. These polymers are charged, and as such, they form an electrostatic barrier around the electrode that can prevent the approach of charged species. Such barriers can aid in 3,4-dihydroxyphenyl-L-alanine (L-DOPA) detection. L-DOPA is used to treat Parkinson's disease but polymerizes on the surface of carbon microelectrodes, forming melanin and acting as an interferent (71). This biofouling is largely mitigated at high concentrations of L-DOPA by electrochemically preconditioning a carbon microfiber electrode and electrodepositing a thin film of Nafion onto the surface of the electrode, maintaining the subsecond response times associated with FSCV (71). Without the Nafion layer, L-DOPA treatment appeared to inhibit the release of DA, but with the Nafion layer, L-DOPA treatment was observed to enhance DA release in neural pathways associated with Parkinson's disease, which highlights the role of electrode design in understanding biochemical pathways in vivo (71).

Direct interference can also be avoided by shifting the potential at which amperometric measurements are made (4, 77–81, 83). Shifting of the needed overpotential can be accomplished by either coating or impregnating the working electrode with dyes, such as Meldola's blue (MB) and Prussian blue (PB). Carbon electrodes modified with MB can be used to monitor enzymatic reactions involving the production of nicotinamide adenine dinucleotide hydrate (NADH) (79). NADH is frequently detected at ~0.6 V, a potential at which AA interferes with these measurements. Incorporation of MB into the electrode shifts the needed potential down to +0.1 V, where AA does not oxidize and thus does not contribute to the measured current. Measuring NADH has been used to diagnose and monitor the intrahepatic cholestasis of pregnancy (79). When diagnosing and monitoring this, it is imperative that biosensors utilizing 3-beta–hydroxysteroid dehydrogenase respond only to analytes of interest because artificially large currents resulting in a false positive could lead to unnecessarily inducing labor.

4.2. Multianalyte Physiometry Utilizing Microdialysate

Monitoring metabolic changes within the brain can help elucidate the biochemical basis of a variety of neural pathologies. Because AA is a known interferent in such experiments, shifting the potential used can help reduce signal overlap with analytes of interest. Secondary enzymes, such as horseradish peroxidase, can be included to shift the potential needed for amperometric

detection of glucose and lactate down to 0.1 V by adding ferrocene to the buffers used to carry the dialysate samples through flow-injection analysis (FIA) systems (4, 75, 80, 81, 84, 85). The use of rapid sampling microdialysis (rsMD) allows for on-line measurements of patient samples in FIA systems (4, 75, 80, 81). When coupled with other methods of monitoring brain activity, such as electrocorticography, correlations can be made between extracellular concentrations of glucose and lactate and spreading depolarizations (SDs) in perilesional tissue following traumatic brain injury (75, 81). After the SD wave passes through the perilesional tissue, significant decreases in glucose and increases in lactate concentrations are noted, likely the result of cellular recovery (81). The observation that the changes in extracellular glucose and lactate concentrations occur after the SD wave has passed suggests that the SD wave is the cause and not the effect of changes in cellular metabolism. For patients experiencing frequent SDs, the extracellular glucose concentration fails to reach pre-SD levels before the next SD, and this prolonged hypoglycemic milieu may contribute to the expansion of the lesion and poor neurologic outcome (81).

As with traumatic brain injuries, localized physiological monitoring after surgical procedures can offer insight into recovery mechanisms as well as provide a personalized approach to medicine to predict patient outcome and alter the course of treatment as necessary. One such procedure is surgical anastomosis, the tethering of tubes or channels such as blood vessels or intestines. Following an anastomosis, the lactate to glucose (L:G) ratio determined through FIA using rsMD may continue to increase near the surgical site, indicating local hypoxia (4, 80). Ischemic conditions, which often require surgical intervention if prolonged, have been evaluated in porcine bowels (80). Using a microdialysis probe intramurally inserted into porcine bowels, the authors measured glucose and lactate both before and after repeated simulated ischemic conditions (80). As ischemia set in, the concentration of glucose decreased with a simultaneous rise in lactate concentration. Upon reperfusion, the levels returned to baseline, but the effects of a secondary ischemic event were more severe than in the first, suggesting that the tissue did not fully recover from the first ischemic event and was more susceptible to future events (80). In such experiments, the ratio of the analytes provides a better picture of the metabolic processes, as slight changes in the position of the microdialysis probe can alter the measurements dramatically. This is in part due to the flushing effect of the microdialysis perfusion fluid over time, which causes artificially decreased absolute concentrations of analytes being measured under conditions in which nutrients are not being replaced, as seen in ischemia.

Monitoring of free flap surgical procedures through FIA with rsMD also predicts patient outcome using the L:G ratio (4). After anastomosis of the arteries and veins of the free flap, the L:G ratio is expected to return to near preoperative baselines as the nutrient supply is restored and wastes are carried away. Cases in which the ratio continued to steadily increase were those when the anastomosis had failed or a thrombosis developed (4). Interestingly, the effect of the topical vasodilator papaverine was also observed in real time: Absolute concentrations of glucose and lactate both increased due to the increase in blood flow to the area (4).

The microdialysis platforms used in these studies have limited temporal resolution in part due to the downstream injection system. However, the use of microdialysis probes is not limited to FIA platforms. Continuous measurements of the microdialysate using traditional enzymatic biosensors can improve temporal resolution (75). In the case of SD wave passages, where the L:G ratio increases (81), on-line sensors are capable of continuously measuring glucose and potassium ion concentrations. Using a potassium ion–selective electrode and the glucose biosensor to monitor induced SD in mice, temporal resolution was improved by a factor of 60, down to 1 s (75). With this method, the decrease in extracellular glucose was temporally resolved from the increase in potassium ion concentration, demonstrating that the drop in glucose is in response to the increased metabolic demands of the neurons undergoing repolarization (75).

4.3. Multianalyte Physiometry Using Implantable Electrodes

Electrodes may also be directly implanted in vivo to probe complex biochemical pathways that are difficult or impossible to reproduce in vitro, such as those seen in the brain. These in vivo electrodes can therefore preserve information about subsecond cellular responses, a daunting task for microdialysis and flow injection methods. However, implanted electrodes present their own set of challenges: The sensitivity of the electrodes must remain constant, and they must be very small or risk a trade-off of spatial resolution for temporal resolution.

Two broad categories of electrodes have proven efficient in maintaining spatial resolution for in vivo physiological measurements: metallic microelectrode arrays (6, 72, 74) and carbon fiber microelectrodes (7, 71, 86–90). Metal microelectrode arrays are slightly larger than carbon fiber electrodes because they spatially separate the surface at which each analyte is detected by electrode-specific functionalization, such as enzymatic or ion-selective films. However, this separation allows for more specific detection of each analyte of interest by decreasing the degree of interference between different analytes while maintaining high sensitivity for individual analytes (6, 72–74, 77, 78, 91). Some metal electrodes are not suitable for implantation despite their ubiquity in in vitro devices. For example, Ag/AgCl film electrodes elicit inflammatory responses in vivo (74). Alternatively, IrO_2 is a biocompatible reference electrode that exhibits long-term stability and low noise in vivo. This electrode is, however, sensitive to pH changes and may only be suitable in regions of the body where pH changes are minimal, such as the brain (74). Metal electrodes have been used to measure physiological changes in the brain in response to mechanical and chemical stimuli. For example, the release of neurotransmitters in the striatum of rats in response to electrical stimuli and physical stresses can be monitored with subsecond temporal resolution using platinum electrodes (6). The second category of implantable electrodes, carbon fiber microelectrodes, has superior spatial resolution relative to metal electrodes. Carbon fiber microelectrodes are frequently used with FSCV to quantitate catecholamines, such as DA (7, 71, 87–89). Because DA adsorbs well to the surface of carbon fiber microelectrodes, faster scan rates are used to maximize signal. Traditionally, this is accomplished by using a triangular waveform, but novel waveforms such as the "sawhorse" scan that briefly holds the potential above +1.0 V further improve sensitivity by opening up sites on the electrode for DA to bind (87). This can be used to deconvolute signals arising from mixtures of redox active molecules, such as adenosine, ATP, and H_2O_2 (92).

Long-term studies with implantable electrodes are limited by their decreased sensitivity over time. Loss of sensitivity is primarily due to biofouling and is compounded by the inability to recalibrate electrodes once implanted (72). Biofouling of glucose oxidase-, lactate oxidase-, and pyruvate oxidase-coated electrodes results in a diffusion barrier shown to decrease sensitivity in vivo (72). However, the purposeful use of diffusion barriers, such as microdialysis membranes, has been shown to extend the linear range of electrodes as well as reduce biofouling. For example, lactate oxidase films protected by a microdialysis membrane better retained sensitivity compared to glucose oxidase and pyruvate oxidase films without the protective membrane (72). Alternatively, FSCV can be used to extend the lifetime of implanted electrodes by eliminating the assumption that the electrode sensitivity is constant during the course of an experiment. It does so by fitting the total background current and switching potential to a model with four regression coefficients (86). This method has accurately predicted the sensitivity of a carbon fiber microelectrode for a variety of analytes in vivo, including DA, AA, H_2O_2, and H^+ (86).

Spatial mapping can be accomplished by electrochemically evaluating how cells respond to different stimuli. Medium spiny neurons can be subtyped by determining how cells respond to DA and the nucleus accumbens mapped in behavioral studies (89). When iontophoresed stimulants are not redox active in the potential range being swept with FSCV, redox active compounds, such as DOPAC (90) and acetaminophen (89), can be added to the iontophoresed solution to

act as internal standards. Glutamate, an iontophoresed stimulant that is not redox active, can be accurately quantified by such internal standards (90).

Responses in different regions of the brain may be seen as the result of a single stimulus by simultaneously using electrodes at different locations (7). For example, DA can be tracked in the nucleus accumbens while 5-HT is tracked in the substantia nigra pars reticulata to investigate the mechanisms governing their release. Upon stimulation, DA release in the nucleus accumbens is 300 times greater than 5-HT release in the substantia nigra pars reticulata, despite their similarity in overall concentration within their respective tissue (7). By selectively inhibiting enzymes responsible for the synthesis, packaging, release, uptake, and metabolism of these two neurotransmitters, the dependence of DA transmission on synthesis and repackaging and the tight regulation of 5-HT transmission by reuptake and degradation pathways were revealed. Additionally, the severe neurological consequences resulting from the coadministration of 5-HT transporter and monoamine oxidase inhibitors were observed (7).

4.4. Wearable Devices for Multianalyte Physiometry

As manageable chronic conditions such as diabetes mellitus, hypertension, and hyperlipidemia become more prevalent, the demand for minimally invasive continuous monitoring devices increases. Wearable devices are now capable of monitoring many different analytes simultaneously, have readouts that interface with mobile phones, and can deliver a therapeutic agent (77). Devices that utilize bodily fluids other than serum and cerebral spinal fluid, such as sweat and urine, are becoming increasingly common in part due to the ease with which samples can be obtained (73, 77, 78, 91). For example, the diabetes patch sits on the surface of the skin, monitors temperature, humidity, pH, and glucose levels, and delivers metformin as needed. In the device, glucose is measured by the amperometric detection of peroxide on gold-doped graphene modified with PB and glucose oxidase at −0.05 V. By using additional sensors to assess pH and temperature, corrections can be made for the activity of glucose oxidase, yielding more accurate glucose readings. When hyperglycemic conditions are detected, a thermal actuator will melt polymeric microneedles incorporating metformin, releasing it into the bloodstream. This patch is capable of continuously monitoring glucose levels over an entire day, and such noninvasive platforms may someday replace current methods of monitoring and managing blood glucose levels.

Wearable MAP microanalytical devices have also been utilized in exercise training regimens to gain insights on individual performance (**Figure 4*c***). Two of the most promising are a three-dimensional (3D)-printed microfluidic device and smart bands. The 3D-printed microfluidic devices have a subcutaneous microdialysis probe that allows external needle-based electrodes to continuously monitor glucose and lactate levels (93). The needle electrodes are removable from the device housing and can be easily modified to measure different analytes as desired. Although technically wearable, this device is still reliant upon an external potentiostat and requires a clinician to subcutaneously insert the microdialysis probe (93). In contrast, a recently developed smart headband/wristband can simultaneously and noninvasively measure glucose, lactate, Na^+, and K^+ levels in sweat (78). In these smart bands, glucose oxidase- and lactate oxidase–chitosan single-walled carbon nanotube films on PB are used for chronoamperometric detection of glucose and lactate, respectively, whereas Na^+ and K^+ levels are determined via open circuit potential using ionophores (Na ionophore X and valinomycin) in ion-selective membranes atop PEDOT:PSS. When access to water is restricted during exercise while wearing the flexible integrated sensor array (FISA), dehydration can be clearly seen when concentrations of sodium and potassium begin to significantly increase. In combination with the real-time profiles of glucose and lactate, athletes undergoing intense training can avoid overexertion and gain physiological insights into individual performance.

Wearable FISAs have also incorporated ion-selective membranes to continuously measure Ca^{2+} and pH levels to determine hydration and electrolyte levels. Ca^{2+} concentration and pH are measured through films incorporating calcium ionophore II on PEDOT:PSS and electropolymerized polyaniline (91). As with sodium and potassium, calcium ion concentration can be monitored with open-circuit potential measurements in sweat during the course of a workout. The in vivo stability of the reference electrode can be enhanced by the incorporation of a polyvinyl butyral layer to maintain chloride ion saturation at the Ag/AgCl film with little interference from other common cations, including NH_4^+, Mg^{2+}, K^+, and Na^+. The results obtained with the FISA for both pH and Ca^{2+} aligned well with the results from commercial pH meters and inductively coupled plasma mass spectrometry (ICP-MS), the gold standard for Ca^{2+} measurement. This indicates that these wearable platforms can be used in clinically relevant conditions, such as hyperparathyroidism and kidney stones.

The quantitation of other metal species bears clinical relevance due to conditions such as Wilson's disease and acute heavy metal poisoning. Heavy metals can be detected by square-wave anodic stripping voltammetry relying on the inherent redox potentials of the metal species being evaluated. The redox potentials of zinc, copper, cadmium, lead, and mercury are sufficiently separated to allow their quantitation in a complex mixture (73). The strong correlation between values obtained from a sweat sample using ICP-MS and the wearable sensor (73) indicates that these wearable sensors can also be used reliably for detection of heavy metals in addition to the aforementioned analytes (78, 91). These advances significantly expand the number of cationic species that can be continuously evaluated in biofluids such as sweat and urine with wearable sensors, thus enlarging the diagnostic toolbox in the field.

5. CONCLUSIONS

The in-house modification of commercially available instruments to convert single-analyte detection systems into those capable of measuring multiple analytes has largely become obsolete in part due to the advent of SPEs and 3D fabrication techniques. The inclusion of customizable sensors in microfluidic devices has enabled multianalyte detection under physiological conditions, allowing researchers to make advances in the fields of bioenergetics, toxicology, and neurology. These devices also show great promise in clinical settings due to their capabilities of continuously monitoring vitals and predicting patient outcome. As the medical field shifts toward more personalized approaches, the widespread adoption of devices that can perform multianalyte detection is inevitable, as evidenced by the continued success of the i-STAT. Outside of research and clinical settings, noninvasive smart bands are beginning to allow athletes to optimize training regimens, and the self-contained nature of these robust fully integrated sensor arrays in combination with their low power usage makes them ideal for use in low-resource monitoring settings as well. The ability to interface these devices with smartphones and computers has the potential to positively impact telemedicine initiatives, as current efforts use analytical signals that are almost entirely physiological (heart rate, temperature) rather than chemical. Overall, multianalyte investigations will continue to grow in number as the monitoring of a panel of analytes is more broadly recognized for its utility to gain a better understanding of fundamental cellular processes and disease states.

DISCLOSURE STATEMENT

The authors are not aware of any affiliations, memberships, funding, or financial holdings that might be perceived as affecting the objectivity of this review.

ACKNOWLEDGMENTS

We thank Dmitry Markov for the photograph of the microclinical analyzer in **Figure 3**.

LITERATURE CITED

1. Bankar SB, Bule MV, Singhal RS, Ananthanarayan L. 2009. Glucose oxidase—an overview. *Biotechnol. Adv.* 27:489–501
2. Mross S, Pierrat S, Zimmermann T, Kraft M. 2015. Microfluidic enzymatic biosensing systems: a review. *Biosens. Bioelectron.* 70:376–91
3. Wang J. 2008. Electrochemical glucose biosensors. *Chem. Rev.* 108:814–25
4. Rogers ML, Brennan PA, Leong CL, Gowers SA, Aldridge T, et al. 2013. Online rapid sampling microdialysis (rsMD) using enzyme-based electroanalysis for dynamic detection of ischaemia during free flap reconstructive surgery. *Anal. Bioanal. Chem.* 405:3881–88
5. Eklund SE, Taylor D, Kozlov E, Prokop A, Cliffel DE. 2004. A microphysiometer for simultaneous measurement of changes in extracellular glucose, lactate, oxygen, and acidification rate. *Anal. Chem.* 76:519–27
6. Wassum KM, Tolosa VM, Wang J, Walker E, Monbouquette HG, Maidment NT. 2008. Silicon wafer-based platinum microelectrode array biosensor for near real-time measurement of glutamate *in vivo*. *Sensors* 8:5023–36
7. Hashemi P, Dankoski EC, Lama R, Wood KM, Takmakov P, Wightman RM. 2012. Brain dopamine and serotonin differ in regulation and its consequences. *PNAS* 109:11510–15
8. McConnell HM, Owicki JC, Parce JW, Miller DL, Baxter GT, Wada HG, et al. 1992. The cytosensor microphysiometer: biological applications of silicon technology. *Science* 257:1906–12
9. Eklund SE, Cliffel DE, Kozlov E, Prokop A, Wikswo J, Baudenbacher F. 2003. Modification of the cytosensor microphysiometer to simultaneously measure extracellular acidification and oxygen consumption rates. *Anal. Chim. Acta* 496:93–101
10. Eklund SE, Snider RM, Wikswo J, Baudenbacher F, Prokop A, Cliffel DE. 2006. Multianalyte microphysiometry as a tool in metabolomics and systems biology. *J. Electroanal. Chem.* 587:333–39
11. Eklund SE, Thompson RG, Snider RM, Carney CK, Wright DW, et al. 2009. Metabolic discrimination of select list agents by monitoring cellular responses in a multianalyte microphysiometer. *Sensors* 9:2117–33
12. Snider RM, McKenzie JR, Kraft L, Kozlov E, Wikswo JP, Cliffel DE. 2010. The effects of cholera toxin on cellular energy metabolism. *Toxins* 2:632–48
13. McKenzie JR, Palubinsky AM, Brown JE, McLaughlin B, Cliffel DE. 2012. Metabolic multianalyte microphysiometry reveals extracellular acidosis is an essential mediator of neuronal preconditioning. *ACS Chem. Neurosci.* 3:510–18
14. Shinawi TF, Kimmel DW, Cliffel DE. 2013. Multianalyte microphysiometry reveals changes in cellular bioenergetics upon exposure to fluorescent dyes. *Anal. Chem.* 85:11677–80
15. Kimmel DW, Dole WP, Cliffel DE. 2013. Application of multianalyte microphysiometry to characterize macrophage metabolic responses to oxidized LDL and effects of an apoA-1 mimetic. *Biochem. Biophys. Res. Commun.* 431:181–85
16. Kimmel DW, Meschievitz ME, Hiatt LA, Cliffel DE. 2013. Multianalyte microphysiometry of macrophage responses to phorbol myristate acetate, lipopolysaccharide, and lipoarabinomannan. *Electroanalysis* 25:1706–12
17. Kimmel DW, Rogers LM, Aronoff DM, Cliffel DE. 2016. Prostaglandin E_2 regulation of macrophage innate immunity. *Chem. Res. Toxicol.* 29:19–25
18. Harry RS, Hiatt LA, Kimmel DW, Carney CK, Halfpenny KC, et al. 2012. Metabolic impact of 4-hydroxynonenal on macrophage-like RAW 264.7 function and activation. *Chem. Res. Toxicol.* 25:1643–51
19. Hiatt LA, McKenzie JR, Deravi LF, Harry RS, Wright DW, Cliffel DE. 2012. A printed superoxide dismutase coated electrode for the study of macrophage oxidative burst. *Biosens. Bioelectron.* 33:128–33
20. Snider RM, Ciobanu M, Rue AE, Cliffel DE. 2008. A multiwalled carbon nanotube/dihydropyran composite film electrode for insulin detection in a microphysiometer chamber. *Anal. Chim. Acta* 609:44–52

21. Weltin A, Slotwinski K, Kieninger J, Moser I, Jobst G, et al. 2014. Cell culture monitoring for drug screening and cancer research: a transparent, microfluidic, multi-sensor microsystem. *Lab Chip* 14:138–46
22. Zeiger SL, McKenzie JR, Stankowski JN, Martin JA, Cliffel DE, McLaughlin B. 2010. Neuron specific metabolic adaptations following multi-day exposures to oxygen glucose deprivation. *Biochim. Biophys. Acta* 1802:1095–104
23. Lizama-Manibusan BN, Klein S, McKenzie JR, Cliffel DE, McLaughlin B. 2016. Analysis of a nitroreductase-based hypoxia sensor in primary neuronal cultures. *ACS Chem. Neurosci.* 7:1188–91
24. McKenzie JR, Cognata AC, Davis AN, Wikswo JP, Cliffel DE. 2015. Real-time monitoring of cellular bioenergetics with a multianalyte screen-printed electrode. *Anal. Chem.* 87:7857–64
25. Lima EA, Snider RM, Reiserer RS, McKenzie JR, Kimmel DW, et al. 2014. Multichamber multipotentiostat system for cellular microphysiometry. *Sens. Actuators B Chem.* 204:536–43
26. Marx V. 2015. Tissue engineering: organs from the lab. *Nature* 522:373–77
27. Wikswo JP, Block FE 3rd, Cliffel DE, Goodwin CR, Marasco CC, et al. 2013. Engineering challenges for instrumenting and controlling integrated organ-on-chip systems. *IEEE Trans. Biomed. Eng.* 60:682–90
28. Witkowska Nery E, Jastrzebska E, Zukowski K, Wroblewski W, Chudy M, Ciosek P. 2014. Flow-through sensor array applied to cytotoxicity assessment in cell cultures for drug-testing purposes. *Biosens. Bioelectron.* 51:55–61
29. Lemaître F, Collignon MG, Amatore C. 2014. Recent advances in electrochemical detection of exocytosis. *Electrochim. Acta* 140:457–66
30. Majdi S, Berglund EC, Dunevall J, Oleinick AI, Amatore C, et al. 2015. Electrochemical measurements of optogenetically stimulated quantal amine release from single nerve cell varicosities in *Drosophila* larvae. *Angew. Chem. Int. Ed.* 54:13609–12
31. Oleinick A, Lemaître F, Collignon MG, Svir I, Amatore C. 2013. Vesicular release of neurotransmitters: converting amperometric measurements into size, dynamics and energetics of initial fusion pores. *Faraday Discuss.* 164:33
32. Amatore C, Delacotte J, Guille-Collignon M, Lemaître F. 2015. Vesicular exocytosis and microdevices—microelectrode arrays. *Analyst* 140:3687–95
33. Li YT, Zhang SH, Wang XY, Zhang XW, Oleinick AI, et al. 2015. Real-time monitoring of discrete synaptic release events and excitatory potentials within self-reconstructed neuromuscular junctions. *Angew. Chem. Int. Ed.* 54:9313–18
34. Bernard A-S, Giroud C, Ching HY, Meunier A, Ambike V, et al. 2012. Evaluation of the anti-oxidant properties of a SOD-mimic Mn-complex in activated macrophages. *Dalton Trans.* 41:6399–403
35. Oliveira R, Bento F, Sella C, Thouin L, Amatore C. 2013. Direct electroanalytical method for alternative assessment of global antioxidant capacity using microchannel electrodes. *Anal. Chem.* 85:9057–63
36. Wang Y, Noel JM, Velmurugan J, Nogala W, Mirkin MV, et al. 2012. Nanoelectrodes for determination of reactive oxygen and nitrogen species inside murine macrophages. *PNAS* 109:11534–39
37. Lu C, Heldt J-M, Guille-Collignon M, Lemaître F, Jaouen G, et al. 2014. Quantitative analyses of ROS and RNS production in breast cancer cell lines incubated with ferrocifens. *Chem. Med. Chem.* 9:1286–93
38. Li Y, Meunier A, Fulcrand R, Sella C, Amatore C, et al. 2016. Multi-chambers microsystem for simultaneous and direct electrochemical detection of reactive oxygen and nitrogen species released by cell populations. *Electroanalysis* 28:1865–72
39. Gunasekara DB, Hulvey MK, Lunte SM. 2011. In-channel amperometric detection for microchip electrophoresis using a wireless isolated potentiostat. *Electrophoresis* 32:832–37
40. Regel A, Lunte S. 2013. Integration of a graphite/poly(methyl-methacrylate) composite electrode into a poly(methylmethacrylate) substrate for electrochemical detection in microchips. *Electrophoresis* 34:2101–6
41. Scott DE, Grigsby RJ, Lunte SM. 2013. Microdialysis sampling coupled to microchip electrophoresis with integrated amperometric detection on an all-glass substrate. *Chem. Phys. Chem.* 14:2288–94
42. Gunasekara DB, Siegel JM, Caruso G, Hulvey MK, Lunte SM. 2014. Microchip electrophoresis with amperometric detection method for profiling cellular nitrosative stress markers. *Analyst* 139:3265–73
43. Lucca BG, Lunte SM, Tomazelli Coltro WK, Ferreira VS. 2014. Separation of natural antioxidants using PDMS electrophoresis microchips coupled with amperometric detection and reverse polarity. *Electrophoresis* 35:3363–70

44. Meneses D, Gunasekara DB, Pichetsurnthorn P, da Silva JA, de Abreu FC, Lunte SM. 2015. Evaluation of in-channel amperometric detection using a dual-channel microchip electrophoresis device and a two-electrode potentiostat for reverse polarity separations. *Electrophoresis* 36:441–48
45. Scott DE, Willis SD, Gabbert S, Johnson D, Naylor E, et al. 2015. Development of an on-animal separation-based sensor for monitoring drug metabolism in freely roaming sheep. *Analyst* 140:3820–29
46. Saylor RA, Reid EA, Lunte SM. 2015. Microchip electrophoresis with electrochemical detection for the determination of analytes in the dopamine metabolic pathway. *Electrophoresis* 36:1912–19
47. Al-Hossaini AM, Suntornsuk L, Lunte SM. 2016. Separation of dynorphin peptides by capillary electrochromatography using a polydiallyldimethylammonium chloride gold nanoparticle-modified capillary. *Electrophoresis* 37:2297–304
48. Lauks IR. 1998. Microfabricated biosensors and microanalytical systems for blood analysis. *Acc. Chem. Res.* 31:317–24
49. Schleicher E. 2006. The clinical chemistry laboratory: current status, problems and diagnostic prospects. *Anal. Bioanal. Chem.* 384:124–31
50. Anderson DJ, Guo B, Xu Y, Ng LM, Kricka LJ, et al. 1997. Clinical chemistry. *Anal. Chem.* 69:165–230
51. Tudos AJ, Besselink GJ, Schasfoort RB. 2001. Trends in miniaturized total analysis systems for point-of-care testing in clinical chemistry. *Lab Chip* 1:83–95
52. Bingham D, Kendall J, Clancy M. 1999. The portable laboratory: an evaluation of the accuracy and reproducibility of i-STAT. *Ann. Clin. Biochem.* 36 (Pt. 1):66–71
53. Hawkes M, Conroy AL, Opoka RO, Namasopo S, Liles WC, et al. 2014. Performance of point-of-care diagnostics for glucose, lactate, and hemoglobin in the management of severe malaria in a resource-constrained hospital in Uganda. *Am. J. Trop. Med. Hyg.* 90:605–8
54. Erickson KA, Wilding P. 1993. Evaluation of a novel point-of-care system, the i-STAT portable clinical analyzer. *Clin. Chem.* 39:283–87
55. Abbott Point of Care Inc. 2015. *i-Stat® system test cartridge menu*. Princeton, NJ: Abbott. **https://www.abbottpointofcare.com/products-services/istat-test-cartridges/menu**
56. Mock T, Morrison D, Yatscoff R. 1995. Evaluation of the i-STAT system: a portable chemistry analyzer for the measurement of sodium, potassium, chloride, urea, glucose, and hematocrit. *Clin. Biochem.* 28:187–92
57. Rudolf J, Douglass J, Baron J, Lewandrowski K. 2015. Evaluation of the i-STAT point-of-care capillary whole blood hematocrit and hemoglobin: comparison to the Siemens RAPIDLab 1200, Sysmex XE5000, and manual spun hematocrit. *Clin. Chim. Acta* 446:37–42
58. MacLeod JA, Nemeth AC, Dicke WC, Wang D, Manalili Wheeler S, et al. 2016. Fast, sensitive point of care electrochemical molecular system for point mutation and select agent detection. *Lab Chip* 16:2513–20
59. Cuartero M, Crespo GA, Bakker E. 2016. Ionophore-based voltammetric ion activity sensing with thin layer membranes. *Anal. Chem.* 88:1654–60
60. Crespo GA, Cuartero M, Bakker E. 2015. Thin layer ionophore-based membrane for multianalyte ion activity detection. *Anal. Chem.* 87:7729–37
61. Cuartero M, Crespo GA, Bakker E. 2016. Polyurethane ionophore-based thin layer membranes for voltammetric ion activity sensing. *Anal. Chem.* 88:5649–54
62. Cuartero M, Crespo GA, Afshar MG, Bakker E. 2014. Exhaustive thin-layer cyclic voltammetry for absolute multianalyte halide detection. *Anal. Chem.* 86:11387–95
63. Grygolowicz-Pawlak E, Crespo GA, Afshar MG, Mistlberger G, Bakker E. 2013. Potentiometric sensors with ion-exchange Donnan exclusion membranes. *Anal. Chem.* 85:6208–12
64. Afshar MG, Crespo GA, Bakker E. 2016. Flow chronopotentiometry with ion-selective membranes for cation, anion, and polyion detection. *Anal. Chem.* 88:3945–52
65. Crespo GA, Ghahraman Afshar M, Bakker E. 2014. Chronopotentiometry of pure electrolytes with anion-exchange Donnan exclusion membranes. *J. Electroanal. Chem.* 731:100–6
66. Afshar MG, Crespo GA, Bakker E. 2014. Counter electrode based on an ion-exchanger Donnan exclusion membrane for bioelectroanalysis. *Biosens. Bioelectron.* 61:64–69
67. Pankratova N, Crespo GA, Afshar MG, Crespi MC, Jeanneret S, et al. 2015. Potentiometric sensing array for monitoring aquatic systems. *Environ. Sci. Process. Impacts* 17:906–14
68. Gauglitz G. 2014. Point-of-care platforms. *Annu. Rev. Anal. Chem.* 7:297–315

69. Gubala V, Harris LF, Ricco AJ, Tan MX, Williams DE. 2012. Point of care diagnostics: status and future. *Anal. Chem.* 84:487–515
70. Pappa AM, Curto VF, Braendlein M, Strakosas X, Donahue MJ, et al. 2016. Organic transistor arrays integrated with finger-powered microfluidics for multianalyte saliva testing. *Adv. Healthc. Mater.* 5:2295–302
71. Qi L, Thomas E, White SH, Smith SK, Lee CA, et al. 2016. Unmasking the effects of L-DOPA on rapid dopamine signaling with an improved approach for nafion coating carbon-fiber microelectrodes. *Anal. Chem.* 88:8129–36
72. Cordeiro CA, de Vries MG, Ngabi W, Oomen PE, Cremers TI, Westerink BH. 2015. *In vivo* continuous and simultaneous monitoring of brain energy substrates with a multiplex amperometric enzyme-based biosensor device. *Biosens. Bioelectron.* 67:677–86
73. Gao W, Nyein HYY, Shahpar Z, Fahad HM, Chen K, et al. 2016. Wearable microsensor array for multiplexed heavy metal monitoring of body fluids. *ACS Sensors* 1:866–74
74. Tolosa VM, Wassum KM, Maidment NT, Monbouquette HG. 2013. Electrochemically deposited iridium oxide reference electrode integrated with an electroenzymatic glutamate sensor on a multi-electrode array microprobe. *Biosens. Bioelectron.* 42:256–60
75. Rogers ML, Feuerstein D, Leong CL, Takagaki M, Niu X, et al. 2013. Continuous online microdialysis using microfluidic sensors: dynamic neurometabolic changes during spreading depolarization. *ACS Chem. Neurosci.* 4:799–807
76. Patel BA, Rogers M, Wieder T, O'Hare D, Boutelle MG. 2011. ATP microelectrode biosensor for stable long-term *in vitro* monitoring from gastrointestinal tissue. *Biosens. Bioelectron.* 26:2890–96
77. Lee H, Choi TK, Lee YB, Cho HR, Ghaffari R, et al. 2016. A graphene-based electrochemical device with thermoresponsive microneedles for diabetes monitoring and therapy. *Nat. Nanotechnol.* 11:566–72
78. Gao W, Emaminejad S, Nyein HY, Challa S, Chen K, et al. 2016. Fully integrated wearable sensor arrays for multiplexed in situ perspiration analysis. *Nature* 529:509–14
79. Lawrance D, Williamson C, Boutelle MG, Cass AEG. 2015. Development of a disposable bile acid biosensor for use in the management of cholestasis. *Anal. Methods* 7:3714–19
80. Córcoles EP, Deeba S, Hanna GB, Paraskeva P, Boutelle MG, Darzi A. 2011. Use of online rapid sampling microdialysis electrochemical biosensor for bowel anastomosis monitoring in swine model. *Anal. Methods* 3:2010
81. Feuerstein D, Manning A, Hashemi P, Bhatia R, Fabricius M, et al. 2010. Dynamic metabolic response to multiple spreading depolarizations in patients with acute brain injury: an online microdialysis study. *J. Cereb. Blood Flow Metab.* 30:1343–55
82. Sansuk S, Bitziou E, Joseph MB, Covington JA, Boutelle MG, et al. 2013. Ultrasensitive detection of dopamine using a carbon nanotube network microfluidic flow electrode. *Anal. Chem.* 85:163–69
83. Lin Y, Liu K, Yu P, Xiang L, Li X, Mao L. 2007. A facile electrochemical method for simultaneous and on-line measurements of glucose and lactate in brain microdialysate with prussian blue as the electrocatalyst for reduction of hydrogen peroxide. *Anal. Chem.* 79:9577–83
84. Jones DA, Parkin MC, Langemann H, Landolt H, Hopwood SE, et al. 2002. On-line monitoring in neurointensive care: enzyme-based electrochemical assay for simultaneous, continuous monitoring of glucose and lactate from critical care patients. *J. Electroanal. Chem.* 538–539:243–52
85. Parkin M, Hopwood S, Jones D, Hashemi P, Landolt H, et al. 2005. Dynamic changes in brain glucose and lactate in pericontusional areas of the human cerebral cortex, monitored with rapid sampling on-line microdialysis: relationship with depolarisation-like events. *J. Cereb. Blood Flow Metab.* 25:402–13
86. Roberts JG, Toups JV, Eyualem E, McCarty GS, Sombers LA. 2013. In situ electrode calibration strategy for voltammetric measurements in vivo. *Anal. Chem.* 85:11568–75
87. Keithley RB, Takmakov P, Bucher ES, Belle AM, Owesson-White CA, et al. 2011. Higher sensitivity dopamine measurements with faster-scan cyclic voltammetry. *Anal. Chem.* 83:3563–71
88. Rodeberg NT, Johnson JA, Cameron CM, Saddoris MP, Carelli RM, Wightman RM. 2015. Construction of training sets for valid calibration of in vivo cyclic voltammetric data by principal component analysis. *Anal. Chem.* 87:11484–91

89. Belle AM, Owesson-White C, Herr NR, Carelli RM, Wightman RM. 2013. Controlled iontophoresis coupled with fast-scan cyclic voltammetry/electrophysiology in awake, freely moving animals. *ACS Chem. Neurosci.* 4:761–71
90. Kirkpatrick DC, McKinney CJ, Manis PB, Wightman RM. 2016. Expanding neurochemical investigations with multi-modal recording: simultaneous fast-scan cyclic voltammetry, iontophoresis, and patch clamp measurements. *Analyst* 141:4902–11
91. Nyein HYY, Gao W, Shahpar Z, Emaminejad S, Challa S, et al. 2016. A wearable electrochemical platform for noninvasive simultaneous monitoring of Ca^{2+} and pH. *ACS Nano* 10:7216–24
92. Ross AE, Venton BJ. 2014. Sawhorse waveform voltammetry for selective detection of adenosine, ATP, and hydrogen peroxide. *Anal. Chem.* 86:7486–93
93. Gowers SA, Curto VF, Seneci CA, Wang C, Anastasova S, et al. 2015. 3D printed microfluidic device with integrated biosensors for online analysis of subcutaneous human microdialysate. *Anal. Chem.* 87:7763–70
94. Honore F, Otis B, Nelson A. 2015. *Reader communication with contact lens sensors and display device*. US Patent No. 20150061837

Annual Review of
Analytical Chemistry

Volume 10, 2017

Contents

Errata

An online log of corrections to *Annual Review of Analytical Chemistry* articles may be found at http://www.annualreviews.org/errata/anchem